Peer Reviewed Paper openaccess Paper Presented at IASIM 2016, July 2016, Chamonix, France

Multivariate data modelling for de-shadowing of airborne hyperspectral imaging

João F. Fortuna[a,*] and Harald Martens[b,c]

[a]Centre for Autonomous Marine Operations and Systems (NTNU AMOS), Department of Engineering Cybernetics, Norwegian University of Science and Technology (NTNU), Trondheim, Norway. E-mail: joao.fortuna@ntnu.no
[b]Department of Engineering Cybernetics, NTNU, Trondheim, Norway
[c]Idletechs AS, Trondheim, Norway

Airborne hyperspectral imaging is a powerful technique for high-resolution classification of large areas of ground, applied today in fields like agriculture and environmental monitoring. Even though many classification algorithms are capable of handling shadows without a decrease in performance, visual inspection can be made easier if shadows are removed. In this paper we present a method for separating the effect of shadows (de-shadowing) and other partially known lighting condition changes from the effects due to the physical, chemical or biological properties of the ground, which are of interest. An example application is shown with good results.

Keywords: airborne, UAV, hyperspectral, de-shadowing, multivariate

Introduction

Outdoors imaging in general, and airborne in particular, suffer from variations in apparent colour caused by illumination and not the reflecting object itself. While this variation may be difficult to correct in RGB images, hyperspectral sensors offer a wealth of redundant data that can be used to remove the effects of different light sources.

Effects of shadows usually represent a multiplicative gain change in reflectance (**R**) data, traditional de-shadowing techniques solve the task by finding the more or less complex gain to compensate for it.[1]

In this paper we present an approach that relies on the multiplicative effect of illumination in reflectance mode, that is, additive in the apparent absorbance [$\log_{10}(1/\mathbf{R})$].

The next section presents the theory behind the method, with all the necessary steps. Following that are the results of the application of the method to airborne hyperspectral data. The last section contains some conclusions and open discussion topics.

The methodology presented here represents an extension of the theory of the informative converse (IC).[2] This theory concerns inadequate mathematical modelling of variations in data from multichannel measurements (Q variables in N samples), and points out how multivariate data modelling can give surprising new insight about unexpected—and thus unmodelled—phenomena in the system measured: it is well known that unmodelled phenomena can lead to alias ("multivariate bias") problems in modelled phenomena's estimated parameters. But the IC theory shows that a subsequent multivariate analysis of the resulting ($N \times Q$) table of unmodelled residuals can give surprisingly good characterisation

Correspondence
J.F. Fortuna (joao.fortuna@ntnu.no)
Received: 31 July 2016
Revised: 8 February 2017
Accepted: 10 February 2017
Publication: 15 February 2017
doi: 10.1255/jsi.2017.a2
ISSN: 2040-4565

Citation
J.F. Fortuna and H. Martens, "Multivariate data modelling for de-shadowing of airborne hyperspectral imaging", *J. Spectral Imaging* **6**, a2 (2017). doi: 10.1255/jsi.2017.a2

of some aspects of the elements missing in the over-simplified modelling. The present paper refines the IC theory by bringing in additional knowledge about the system at hand.

As mentioned, established approaches try to estimate changes in intensity *gain* in order to compensate for shadows in hyperspectral image data. Let the data matrix $\mathbf{Y}(N \times Q)$ be a table of transformed spectra (N pixels, Q wavelength channels), obtained by treating the multi-channel spectral data in the N pixels as if they represented Q-dimensional spectra from a spectrophotometer: reflected intensity from a scene is observed by the camera ($\mathbf{I}$). For gain control, each pixel's measured $\mathbf{I}$ is element-wise divided by $\mathbf{I}_0$, the reflected intensity of a white body with the same light source, to convert $\mathbf{I}$ to reflectance ($\mathbf{R}$). Finally, the linearised data are given by the apparent absorbance $\mathbf{Y} = \log_{10}(1/\mathbf{R})$.

Hence, in order to ensure that systematic variations in $\mathbf{I}_0$ can be modelled additively instead of multiplicatively, we replace the camera's intensity measurements $\mathbf{I}$ by the apparent absorbance, $\mathbf{Y} = \log_{10}(1/\mathbf{R})$ in the subsequent multivariate spectral modelling.

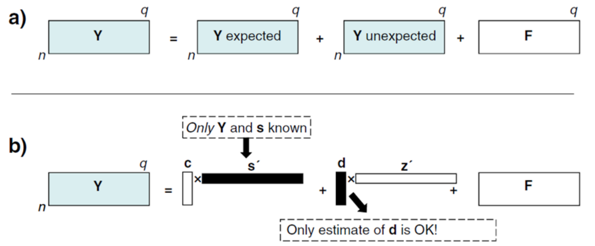

Figure 1. The informative converse paradox, illustrated for a linear model of the two constituents, observed in Y**(*N* × *Q*) at *Q* wavelengths in *N* pixels;** Y**(*n* × *q*) is the original notation from Reference 2. a) The measurements** Y **have both an expected and an unexpected source contribution, in addition to random measurement errors** F**. b) The expected and unexpected source contributions may be modelled as** c × s′ **and** d × z′**, respectively. When only measurements** Y **and the expected source's known spectrum** s **are known, while its concentration** c **and unexpected concentration** d **and spectrum** z **are unknown, the original IC method gives a surprisingly good estimate of the unexpected** d**, but erroneous (aliased) estimates both for the expected** c **and the unexpected** z**. (Adapted from Reference 2 and reproduced with the permission of the publisher).**

The informative converse paradox

Figure 1 illustrates the original IC paradox. The basic problem is illustrated in Figure 1a): measured data $\mathbf{Y}$ often represent the sum of two causal sources—expected and unexpected ones—plus random errors ($\mathbf{F}$). The unexpected variation sources can seriously interfere with the modelling of $\mathbf{Y}$. For instance, assume that the spectral data $\mathbf{Y}$ have contributions from an expected phenomenon with spectral profile $\mathbf{s}$ and levels $\mathbf{c}$ in n pixels, plus contributions from an unexpected phenomenon with spectral profile $\mathbf{z}$ and levels $\mathbf{d}$ in the n pixels:

$$\mathbf{Y} = \mathbf{cs}' + \mathbf{dz}' + \mathbf{F} \tag{1a}$$

where $\mathbf{Y}(N \times Q)$: hyperspectral reflectance measurements for N pixels (rows) at Q different wavelength channels (columns), linearised as $\log_{10}(1/\mathbf{R})$; $\mathbf{cs}' = \mathbf{c}(N \times 1)\,\mathbf{s}'(1 \times Q)$: contributions from a partially known cause; $\mathbf{dz}' = \mathbf{d}(N \times 1)\,\mathbf{z}'(1 \times Q)$: contributions from a totally unknown; $\mathbf{F}(N \times Q)$: measurement and modelling errors (assumed, for simplicity, to be random, normally distributed).

If the spectral data in $\mathbf{Y}$ are modelled inadequately (Figure 1b) in terms of known spectrum $\mathbf{s}$ only, while $\mathbf{z}$ is ignored, the estimate of $\mathbf{c}$ [e.g. $\hat{\mathbf{c}} = \mathbf{Ys}(\mathbf{s}'\mathbf{s})^{-1}$] will be contaminated by contributions from $\mathbf{d}$ and thus "unnatural". But the IC *paradox* (Figure 1b) is that a subsequent multivariate PCA analysis of $\mathbf{Y} - \hat{\mathbf{c}}\mathbf{s}'$ yields estimates of $\mathbf{d}$ with the correct, "natural" expectancy (except for a trivial scaling factor). The corresponding estimate of $\mathbf{z}$ from that PCA will be "unnatural" due to its orthogonality to $\mathbf{s}$.

The present paper modifies this IC methodology by correcting the estimates of $\mathbf{c}$ and $\mathbf{z}$ with the use of additional assumptions (non-negativity etc.), extends it to multicomponent models and applies it to hyperspectral airborne images of ground scenes in order to separate illumination changes (shadows etc.) and ground properties (geology, vegetation etc.).

In the following we show that shadow effects and illumination changes may be expected to give additive phenomena, allowing us to write the following multivariate linear model:

$$\mathbf{Y} = \mathbf{CS}' + \mathbf{DZ}' + \mathbf{F} \tag{1b}$$

For hyperspectral data $\mathbf{Y}$ each matrix takes the meaning below:

$\mathbf{Y}(N \times Q)$: hyperspectral absorbance for N pixels (rows) at Q different wavelength channels (columns), linearised as $\mathbf{Y} = \log_{10}(1/\mathbf{R})$;
$\mathbf{CS}' = \mathbf{C}(N \times J)\,\mathbf{S}'\ (J \times Q)$: expected contributions from partially known causes (e.g. light sources);
$\mathbf{DZ}' = \mathbf{D}(N \times M)\mathbf{Z}'\ (M \times Q)$: unexpected contributions from totally unknown causes (e.g. ground components);
$\mathbf{F}(N \times Q)$: measurement and modelling errors (assumed, for simplicity, to be random, normally distributed).

It is, of course, possible to estimate the expected sources' unknown concentration parameters $\mathbf{C}(N \times J)$ of J constituents in N pixels from their known spectra $\mathbf{S}(Q \times J)$, using the over-simplified linear model ignoring the unexpected variation source(s) $\mathbf{DZ}'$:

$$\mathbf{Y} = \mathbf{CS}' + \mathbf{F} \tag{1c}$$

But since this represents an over-simplified mathematical model of reality, it can give serious errors in the parameters identified—in this case the estimates of $\mathbf{C}$ from $\mathbf{S}$ only. The purpose of present paper is to give good estimates also of the expected source's pixel levels $\mathbf{C}$ and the unexpected sources' contribution levels $\mathbf{D}$ and spectra $\mathbf{Z}$ as well as residuals $\mathbf{F}$ in such cases.

Method

The IC modelling extension may be applied in different ways. For illustration, we here assume that $\mathbf{Z}$, the spectral properties of the main ground constituents (plants, rocks, water etc.) are unknown, and so are their pixel-by-pixel level ("concentration") variations $\mathbf{D}$, while $\mathbf{S}$, the spectra of possible lighting conditions (sunlight, overcast etc.), is known, while their pixel-by-pixel level variations $\mathbf{C}$ are unknown. But the presented method also works in the converse case, when only $\mathbf{C}$ is known, while their spectra $\mathbf{S}$ are unknown (see Reference 2). Likewise, the method may be used to estimate and correct for the spectral effects of unknown light sources, particularly if the spectral properties or the pixel-by-pixel level variations of some or all of the main ground components are known. Necessary modifications to the algorithm are trivial and will not be explained here.

Relating the unknowns to the known or easily estimated parameters

We can always express the spectra $\mathbf{Z}$ and levels $\mathbf{C}$ as function of the spectra $\mathbf{S}$ and levels $\mathbf{D}$, respectively:

$$\mathbf{Z} = \mathbf{SA} + \mathbf{Z}_{\perp\mathbf{S}} \tag{2a}$$

$$\mathbf{C} = \mathbf{DB} + \mathbf{C}_{\perp\mathbf{D}} \tag{2b}$$

where $\mathbf{A}(J \times M)$ and $\mathbf{B}(M \times J)$ represent the coupling of unexpected spectra $\mathbf{Z}$ to known spectra $\mathbf{S}$ and expected but unknown levels $\mathbf{C}$ to unexpected levels $\mathbf{D}$, respectively. The M-dimensional subspace of $\mathbf{D}$ is easy to estimate by IC analysis.[2] If all elements in $\mathbf{A}$ (or $\mathbf{B}$) are 0, $\mathbf{Z}$ and $\mathbf{S}$ (or $\mathbf{C}$ and $\mathbf{D}$) are orthogonal, the alias problem disappears. If not, then they represent spectral- and/or level-overlaps that will create alias errors unless estimated and compensated for.

Summary model of the overlap between the expected and unexpected signal contributions

$$\begin{aligned}\mathbf{Y} &= \mathbf{CS}' + \mathbf{DZ}' + \mathbf{F} \\ &= (\mathbf{DB} + \mathbf{C}_{\perp\mathbf{D}})\mathbf{S}' + \mathbf{D}(\mathbf{A}'\mathbf{S}' + \mathbf{Z}'_{\perp\mathbf{S}}) + \mathbf{F} \\ &= \mathbf{D}(\mathbf{B} + \mathbf{A}')\mathbf{S}' + \mathbf{C}_{\perp\mathbf{D}}\mathbf{S}' + \mathbf{DZ}'_{\perp\mathbf{S}} + \mathbf{F} \\ &= \mathbf{DHS}' + \mathbf{C}_{\perp\mathbf{D}}\mathbf{S}' + \mathbf{DZ}'_{\perp\mathbf{S}} + \mathbf{F}\end{aligned} \tag{3}$$

where $\mathbf{H}(M \times J)$ is the sum of the unknown ambiguity matrices in $\mathbf{Z}$ (w.r.t. $\mathbf{S}$) and $\mathbf{C}$ (w.r.t. $\mathbf{D}$):

$$\mathbf{H} = \mathbf{B} + \mathbf{A}' \tag{4}$$

Estimation methodology

In the following steps, ordinary least squares (OLS) regression is used in all estimations. If different input variables (columns in $\mathbf{Y}$) are known to have different relevance or reliability, then the OLS may be replaced by weighted least squares (WLS) or generalised least squares (GLS) in all the regressions over channels. Likewise, if different pixels (rows in $\mathbf{Y}$) need different weights, then WLS or GLS regression may be used in all regressions over observations. Alternatives to OLS/WLS/GLS, such as best linear unbiased predictors (BLUP) or robust statistical estimators etc., may also be used.

Estimation of model parameters

- $\mathbf{S}$ is assumed known
- $\mathbf{D}$ and $\mathbf{Z}_{\perp\mathbf{S}}$ are easy to estimate by the IC analysis:[2]

$$\hat{\mathbf{C}}_{Prelim} = \mathbf{YS}(\mathbf{S}'\mathbf{S})^{-1} \tag{5a}$$

$$\mathrm{E}(\hat{\mathbf{C}}_{Prelim}) = \mathbf{C} + \mathbf{DA}' \tag{5b}$$

$$\mathbf{F}_{IC} = \mathbf{Y} - \hat{\mathbf{C}}_{Prelim}\mathbf{S}' \tag{6a}$$

$$\mathrm{E}(\mathbf{F}_{IC}) = \mathbf{DZ}'_{\perp\mathbf{S}} \tag{6b}$$

Singular value decomposition (SVD) of the IC residual $\mathbf{F}_{IC}$ gives, for its q most significant components:

$$[\mathbf{U}_{IC}, \mathbf{s}_{IC}, \mathbf{V}_{IC}] = \mathrm{svd}(\mathbf{F}_{IC}, q) \tag{7}$$

which yields estimates of the bilinear structure $\mathbf{DZ}_{\perp \mathbf{S}}$. With

$$\hat{\mathbf{D}} = \mathbf{U}_{IC}\mathrm{diag}(\mathbf{s}_{IC}) \tag{8}$$

$$\hat{\mathbf{Z}}_{\perp \mathbf{S}} = \mathbf{V}_{IC} \tag{9}$$

■ $\mathbf{C}_{\perp \mathbf{D}}$ is estimated by:

$$\hat{\mathbf{C}}_{\perp \mathbf{D}} = \left[\mathbf{I} - \hat{\mathbf{D}}\left(\hat{\mathbf{D}}'\hat{\mathbf{D}}\right)^{-1}\hat{\mathbf{D}}\right]\hat{\mathbf{C}}_{Prelim} \tag{10}$$

Estimating the ambiguity matrix H

$$\mathbf{Y} = \mathbf{DHS}' + \mathbf{C}_{\perp \mathbf{D}}\mathbf{S}' + \mathbf{DZ}'_{\perp \mathbf{S}} + \mathbf{F} \tag{11a}$$

$$\mathbf{DHS}' = \mathbf{Y} - \mathbf{C}_{\perp \mathbf{D}}\mathbf{S}' - \mathbf{DZ}'_{\perp \mathbf{S}} - \mathbf{F} \tag{11b}$$

Insert estimates:

$$\hat{\mathbf{D}}\mathbf{HS}' \approx \mathbf{Y} - \mathbf{C}_{\perp \mathbf{D}}\mathbf{S}' - \mathbf{DZ}'_{\perp \mathbf{S}} \tag{12}$$

Solve to estimate $\mathbf{H}$:

$$\hat{\mathbf{H}} = \left(\hat{\mathbf{D}}'\hat{\mathbf{D}}\right)^{-1}\hat{\mathbf{D}}'\left(\mathbf{Y} - \hat{\mathbf{C}}_{\perp \mathbf{D}}\mathbf{S}' - \hat{\mathbf{D}}\mathbf{Z}'_{\perp \mathbf{S}}\right)\mathbf{S}\left(\mathbf{S}'\mathbf{S}\right)^{-1} \tag{13}$$

Figure 2. RGB reconstruction of original data.

Estimation of expected source levels C and unexpected spectra Z

From Equations 2 and 4:

$$\begin{aligned}\hat{\mathbf{C}} &= \hat{\mathbf{D}}\left(\hat{\mathbf{H}} - \mathbf{A}'\right) + \hat{\mathbf{C}}_{\perp \mathbf{D}} \\ &= \hat{\mathbf{D}}\hat{\mathbf{H}} + \hat{\mathbf{C}}_{\perp \mathbf{D}} - \hat{\mathbf{D}}\mathbf{A}'\end{aligned} \tag{14}$$

$$\begin{aligned}\hat{\mathbf{Z}} &= \hat{\mathbf{S}}\left(\hat{\mathbf{H}}' - \mathbf{B}'\right) + \hat{\mathbf{Z}}_{\perp \mathbf{S}} \\ &= \hat{\mathbf{S}}\hat{\mathbf{H}}' + \hat{\mathbf{Z}}_{\perp \mathbf{S}} - \mathbf{SB}'\end{aligned} \tag{15}$$

Hence, $\hat{\mathbf{C}}$ (and $\hat{\mathbf{Z}}$) have unknown matrices $\mathbf{A}(J \times M)$ [and $\mathbf{B}(M \times J)$], which describe how $\mathbf{Z}$ depends on $\mathbf{S}$ (how $\mathbf{C}$ depends on $\mathbf{D}$), and that generates ambiguity w.r.t. $\hat{\mathbf{D}}$ (and $\mathbf{S}$). This ambiguity can only be eliminated by additional information about $\mathbf{C}$ (and $\mathbf{Z}$) (e.g. non-negativity, unimodality, smoothness, ICA based on entropy etc.).

Estimation of spectral overlap A and level overlap B

By applying previous knowledge about $\mathbf{C}$ and $\mathbf{Z}$ such as smoothness, $\mathbf{A}$ and $\mathbf{B}$ can be estimated by an optimiser, for instance YALMIP.[3]

Since only the product $\mathbf{DZ}'$ can be estimated from $\mathbf{Y}$ and $\mathbf{S}$, the individual matrices $\mathbf{D}$ and $\mathbf{Z}$ need to be determined by methods such as MCR-ALS.[4]

Results

Applying the method to airborne hyperspectral images yields promising results. Here, we borrowed sample data

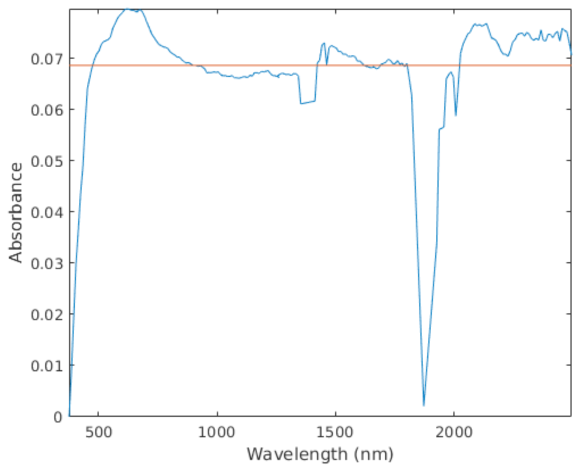

Figure 3. Estimated spectra of known lighting effects (S): a constant "baseline" and a shadow signature (here estimated from sunny vs shaded mountain sides).

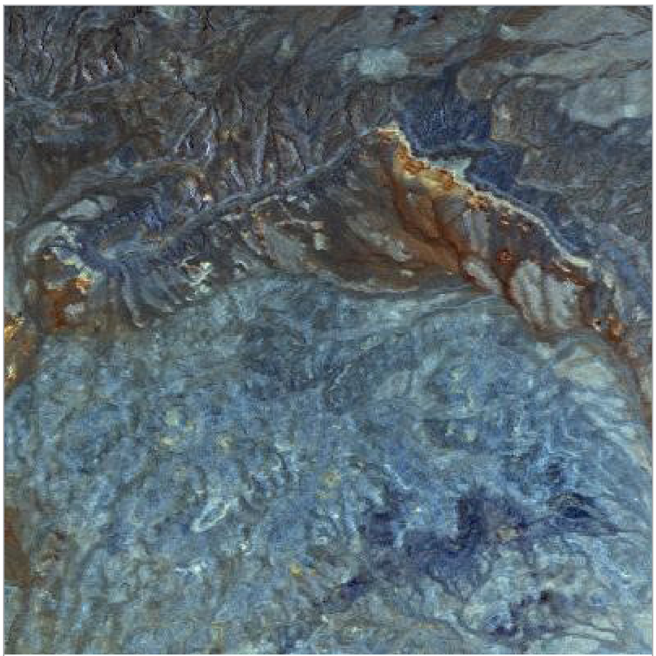

Figure 4. De-shadowed data, given as RGB.

Figure 5. Shadow data, given as RGB. 10 principal components were used for the estimation of the de-shadowed data.

from NASA's AVIRIS programme,[5] see Figure 2. This is a visible/NIR instrument, measuring reflected light at wavelengths from 400 nm to 2500 nm. Some noisy bands were removed.

RGB images were generated using a weighted sum of spectral channels in the visible range, in a similar fashion to the spectral response of the human eye. For this, we ensured data were in reflectance mode. The weights for the weighted sum were calculated using Gaussian curves centred on the most peak wavelengths of the cone cells in the human eye, such wavelengths are well known and easily available.[6]

S was simplified to two spectra, given in Figure 3, the skylight spectrum was estimated by taking the difference of spectra between pixels in shadow and light regions in small neighbourhoods (so that the ground effects are expected to be the same).

Figure 4 shows the de-shadowed data, at first glance it seems as if all the terrain information was removed, like a flattened version of the original data. On the other hand, the "shadow map" in Figure 5 appears to contain only terrain information and nothing about the different constituents of the ground. Both de-shadowed and shadow data hold valuable information, chemistry/geology and physics/topology, respectively.

By comparing the performance of a simple *k-means* clustering (chosen number of clusters = 3) on the original (Figure 6) and de-shadowed (Figure 7) data, we can see how the effect of shadows and morphology is removed and clusters are based on ground "chemistry". Increasing the number of clusters beyond three revealed more interesting ground features (not shown here).

Conclusions

Theoretically, the extended IC method presented here seems able to simplify the interpretation of hyperspectral images by better "de-shadowing": improved separation of light source variations from ground property variations. Using additional assumptions, such as spatial ground topology or other known ground or light source features, both expected and unexpected signal sources can thus be quantified rather completely—or at least with less alias errors—compared to the original IC method without such assumptions.

For instance, in the hyperspectral aerial image illustrated, the extended IC attained good "de-shadowing" by the use of additional assumption about where to discover the light source spectrum **s** (in this case the contrasts between sunny and shaded sides of mountains). Some features that appear in the de-shadowed RGB representation of the image (Figure 4) are not apparent

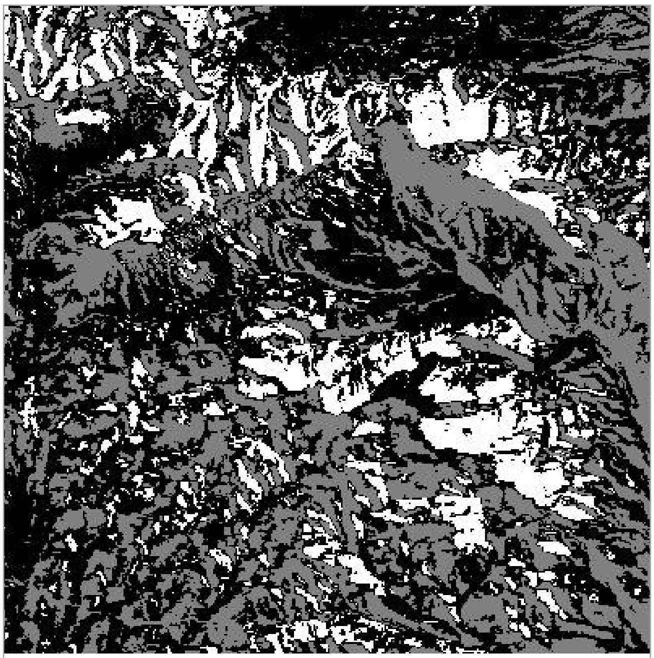

Figure 6. Clustering in original data.

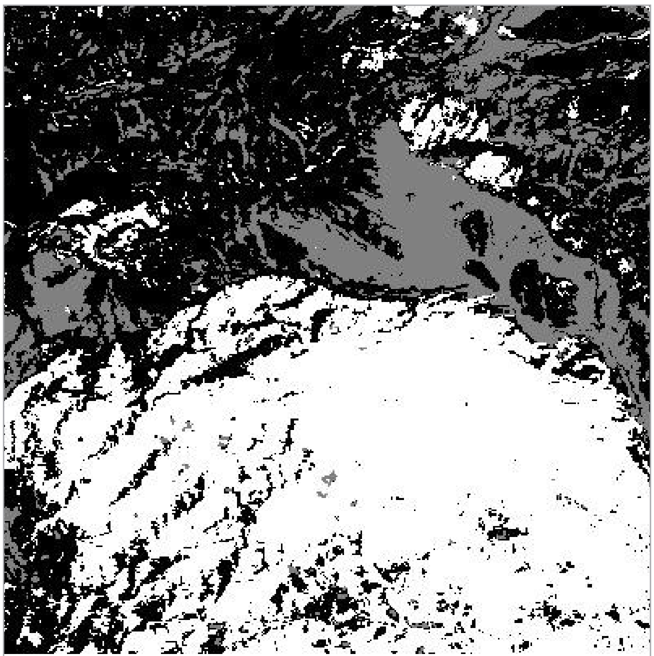

Figure 7. Clustering in de-shadowed data.

in Figure 2. A dark patch in the lower-right area of the picture is particularly noticeable. One may hypothesise that the information was contained in the NIR bands which was not showing in the original RGB reconstruction, but when removing the effects of illumination it was made more evident.

Hence, the extended IC method resolved some of the paradox in the original IC. We believe that the new method can simplify the human interpretation as well as the automated quantitative use of hyperspectral imaging. Work is in progress to improve the method optimisation step further.

References

1. S. Adler-Golden, M.W. Matthew, G.P. Anderson, G.W. Felde and J.A. Gardner, "An algorithm for de-shadowing spectral imagery", in *AVIRIS Earth Sciences and Applications Workshop* (2002).
2. H. Martens, "The informative converse paradox: windows into the unknown", *Chemometr. Intell. Lab. Syst*. **107(1),** 124–138 (2011). doi: https://doi.org/10.1016/j.chemolab.2011.02.007
3. J. Löfberg, "YALMIP: a toolbox for modeling and optimization in MATLAB", in *CACSD Conference*, Taipei, Taiwan (2004).
4. J. Jaumot, A. de Juan and R. Tauler, "MCR-ALS GUI 2.0: New features and applications", *Chemometr. Intell. Lab. Syst*. **140,** 1–12 (2015). doi: https://doi.org/10.1016/j.chemolab.2014.10.003
5. NASA JPL, *AVIRIS Data Portal* [online]. Available at http://aviris.jpl.nasa.gov/alt_locator/. [Accessed June 2016].
6. Wikipedia, *Color Vision* [Online]. Available at https://en.wikipedia.org/wiki/Color_vision. [Accessed June 2016].